Indonesian Journal of Pharmacy

VOL 36 (4) 2025: 777–787 | RESEARCH ARTICLE

In Vitro Evaluation of 4-Methoxyresorcinol and Kaempferol 7-*O*-Rutinoside and Their Radioiodinated Derivatives in MCF-7, MDA-MB-231, and LNCaP Cell Lines

Hendris Wongso[1*], Putri Rochmantika[2] , Alfian M. Forentin[1], Veronika Y. Susilo[1], Muhamad B. Febrian[1], Isa Mahendra[1], Ahmad Kurniawan[1], Crhisterra E. Kusumaningrum[1], Asep Rizaludin[3], Yanuar Setiadi[4] and Ari S. Nugraha[2*]

1. Research Center for Radioisotope, Radiopharmaceutical, and Biodosimetry Technology, Research Organization for Nuclear Energy, National Research and Innovation Agency of the Republic of Indonesia, Tangerang Selatan, Banten 15314, Indonesia
2. Drug Utilisation and Discovery Research Group, Faculty of Pharmacy, Universitas Jember, Jember 68121, Indonesia
3. Research Center for Radioisotope, Radiopharmaceutical, and Biodosimetry Technology, Research Organization for Nuclear Energy, National Research and Innovation Agency of the Republic of Indonesia, Tangerang Selatan, Banten 15314, Indonesia
4. Research Center for Computing, Research Organization for Electronics and Informatics, National Research and Innovation Agency, Bandung, Jawa Barat 40135, Indonesia

Article Info

Submitted: 28-11-2023
Revised: 19-10-2024
Accepted: 20-10-2024

*Corresponding author
Hendris Wongso,
Ari Satia Nugraha

Email:
hend042@brin.go.id
arisatia@unej.ac.id

ABSTRACT

The global population is currently experiencing high rates of mortality due to the growing burden of cancer. Efforts on the development of new potent anticancer agents are necessary. Therefore, this study aimed to evaluate the anticancer activity of two flavonoids, including 4-methoxyresorcinol (MRC) and kaempferol 7-*O*-rutinoside (K7R), isolated from *Melia azedarach* L. leaves. Anticancer activity was evaluated in vitro against MCF-7, MDA-MB-231, and LNCaP cell lines. Radioiodination was performed with iodine-131 as well as computational studies to assess the feasibility of the isolated compounds as natural product-based radiopharmaceuticals for diagnosing and managing cancer. The results showed that MRC and K7R had moderate anticancer activity against MCF-7, MDA-MB-231, and LNCaP cell lines with IC_{50} values ranging from 154.75 to 1962.66 µM. Cellular uptake investigations found that the highest cellular accumulation of [^{131}I]-4-methoxyresorcinol (MRCI) was observed in MCF-7 (3.17 ± 0.11%) after 24 hours of incubation, approximately 20-fold greater than the control group uptake (iodine-131). Meanwhile, [^{131}I]-kaempferol 7-*O*-rutinoside (K7RI) showed the highest uptake in MCF-7 (3.05 ± 0.9%) post-one hour of incubation, which was around 23-folds higher than iodine-131 uptake. In conclusion, both MRC and K7R were identified as potential anticancer drugs, which could be further developed into new radiopharmaceutical candidates.

Keywords: *Melia azedarach* L., Anticancer, Radioiodination, Cellular uptake, Computational analysis

INTRODUCTION

Cancer is a growing disease burden that causes high morbidity and mortality numbers among global populations (J. Zhao et al., 2023). There are some therapeutics available for managing cancer, including surgery, chemotherapy, and radiation therapy which has been used in a single form or in combination. More recently, progress in combating cancer has been achieved by using multiple targeted therapies with a synergistic effect (Debela et al., 2021). The development of radiopharmaceuticals for cancer diagnosis and management is an actively expanding field. Radiopharmaceuticals can be used for noninvasive imaging of the anatomical and physiological events in cancer, as well as

neurodegenerative, cardiovascular, and endocrine diseases. For therapeutic purposes, the radiopharmaceuticals are commonly used to manage various cancer types (Petrov et al., 2022).

Many radiopharmaceuticals are developed from different active substances, such as small organic compounds, peptides, nanoparticles, proteins, and antibodies. Recently, several natural bioactive compounds have been used as building blocks or ligands for the manufacture of diagnostic or therapeutic radiopharmaceuticals (Wongso, 2022). The role of natural products as sources of therapeutic molecules to prevent and control human diseases is reported in several studies. Despite the numerous applications of natural products in pharmaceutical and medicinal fields, plant-derived drugs are often used as alternatives to modern medicines for many reasons (Atanasov et al., 2021; Nasim et al., 2022; Rizvi et al., 2022). Among natural compound classes, flavonoids are an important group of products well known for the health benefits as antioxidant, anti-inflammatory, anti-mutagenic, and anticancer (Panche et al., 2016). In addition, flavonoids are the the most diverse secondary metabolite class compounds across the plant kingdom in which the abudance has become feasible starter for natural-based products from nutraceutical to pharmaceuticals. Therefore, flavonoids are used as chemical scaffolds as well as alternative sources for the development of various drugs (Tungmunnithum et al., 2018; Ullah et al., 2020).

Indonesia as an archipelago country consists of around 17,508 islands and is covered by various vegetations as well as marine environments. This country has been found to contain approximately 6,000 plants identified as species with medicinal prospects (Hanif et al., 2019; Nugrahaa & Keller, 2011). Mindi (*Melia azedarach* L.) is among the Indonesian plants tradionally used to manage various ailments, including stomatch pain, diabetes, headaches, and diarrhea. Previous investigations reported some phenolics from the leaves extract of *M. azedarach*, and the potential of the crude extract against prostate cancer cell lines (LNCaP) as well as breast cancer (MDA-MB-231 and MCF-7). In this study, there was further exploration of the phenolics constituents isolated from *M. azedarach* and the potential application in modern medicine as suitable scaffold for the development of new radiopharmaceuticals (Nugraha et al., 2023).

Based on the explanation above, this study aimed to evaluate the anticancer activity of two phenolics compounds, namely 4-methoxyresorcinol (MRC) and kaempferol 7-*O*-rutinoside (K7R), isolated from Indonesian *M. azedarach* leaves. Additionally, the prospect of the compounds as new radiopharmaceutical candidates was evaluated in cellular uptake and computational studies.

MATERIAL AND METHOD

Materials and Instruments

All chemicals used in this study without further purification were laboratory or reagent grade. Isolation and characterization of MRC and K7R from *M. azedarach* was accomplished in the previous investigation (Nugraha et al., 2023). NaI-131 solution was produced by the G.A. Siwabessy Multi-Purpose Reactor, Directorate of Nuclear Facility Management, and subsequently prepared by the Radioisotope Research Group at the Research Center for Radioisotope, Radiopharmaceutical, and Biodosimetry Technology, National Research and Innovation Agency of Indonesia (BRIN).

Cell Culture Preparation

Several cell lines were used to evaluate the biological activity of MRC and K7R isolated from *M. azedarach*. The LNCaP was acquired from the European Collection of Authenticated Cell Cultures (ECACC) as a representative of human prostate cancer. Additionally, the MDA-MB-231 and MCF-7 were procured from the American Type Culture Collection (ATCC) as models of human breast cancer. All cell lines were grown and prepared under optimum conditions. For cultivation, 10% fetal bovine serum (Gibco), penicillin (100 I.U/mL), streptomycin (100 µg/mL) (Gibco), amphotericin B (2.5 µg/mL) (Gibco), and 10 mM sodium pyruvate (Gibco) were added to RPMI 1640 medium (Gibco). Cells were stored in culture incubators at 37°C, 5% CO_2, and approximately 95% relative humidity (RH) until the preparation for in vitro assay.

Cytotoxicity Assay

The MTT reagent, namely 3-(4,5-Dimethylthiazol-2-yl)-2,5-Diphenyltetrazolium Bromide, was used to investigate the cytotoxic potential of MRC and K7R on LNCaP, MDA-MB-231, and MCF-7 cell lines. This method was described by Mossman (Mosmann, 1983), and modified slightly for the current study. Harvesting and seeding was conducted at a density of 1.5 x 10^4 cells per well in 96-well microplates with flat bottom. Furthermore, cells were grown until a confluence of greater than

80% was reached. Both MRC and K7R were dissolved in dimethyl sulfoxide (DMSO). The samples were prepared under aseptic conditions at various concentrations, ranging from 42.05 to 336.41 µM (K7R) and 178.40 to 1783.97 µM (MRC) in the growth medium. Cells were treated with the samples for 24 hours in triplicate to obtain a set of sample concentrations. The control cells were divided into two groups, among which one was cultivated using DMSO in the medium and the other in the absence of DMSO. After incubation was complete, the growth medium was discarded, and the cells were rinsed twice with phosphate-buffered saline (PBS). An equal amount of 100 µL of medium containing 0.5 mg/mL of MTT reagent was added to each well, including the control. Two to four hours were spent incubating the plate in an incubator set to 37°C with a 5% CO_2 atmosphere. Approximately 100 µL of a 10% SDS solution was added post formazan crystal formation. The cell viability was determined using a microplate reader to measure the absorbance at 570 nm. The IC_{50} values and graphs were generated with GraphPad Prism Version 9.0.0, while the statistical analysis was performed using a one- or two-way analysis of variance (ANOVA) test.

Cellular Uptake assay

Cellular uptake study of [^{131}I]-4-methoxyresorcinol (MRCI) and [^{131}I]-kaempferol 7-*O*-rutinoside (K7RI) was carried out against LNCaP, MDA-MB-231, and MCF-7 cell lines. Seeding was conducted at a density of 5.0 x 10^4 cells per well in 24-well flat-bottom microplates. Cells were grown until a confluence of greater than 80% was reached. All growth medium was removed, and cold PBS was used for washing cell cultures. The radiolabelled compounds were prepared under aseptic conditions and diluted in HBSS. Subsequently, 37 kBq of samples in 500 µL of HBSS were added to each well containing cells and incubation was performed in quadruplicate for a set of time intervals including 0.25, 0.50, 1.0, 2.0, 3.0 and 24 hours. When the incubation period completed, the solution was collected, the cells were rinsed with 500 µL of HBSS, and recollected in the same tube, representing the uninternalized fraction. Furthermore, the cells were lysed with 300 µL of a 0.2 N NaOH solution, rinsed with 500 µL of HBSS, and collected in a tube as lysate, representing the internalized fraction. The gamma counter was used to measure the amount of radiation in each fraction. By comparing the radioactivity in the lysate to the standard radioactive solution, the percentage of cellular uptake was calculated. The GraphPad Prism 9.0.0 programme was used for the graph and statistical analysis.

Radiolabelling

The radioiodinated forms of MRC and K7R were synthesized through direct radioiodination procedure under acidic conditions (pH = 5-6) as previously reported, with some minor variations (Wongso et al., 2022). Chloramine-T solution (0.1 mg) in 100 µL H_2O was added to each compound (0.1 mg) in DMSO (100 µL), followed by a slow introduction of NaI-131 solution (± 1.85 MBq) and acetic acid 50% (10 µL). The reaction mixture was incubated and shaken at 700 rpm for 30 minutes at 25 °C. The 0.5 M $Na_2S_2O_5$ (50 µL) solution was added, and the reaction was shaken for another 2 minutes to generate the corresponding products. Subsequently, the radiochemical purity (RCP) was determined by radio-TLC using TLC-SG F60 paper chromatography (0.5 x 8 cm) as a stationary phase. The mixture of dichloromethane (DCM) and methanol (MeOH) (9:1, v/v) was used as a mobile phase. The first and second radiochromatograms represent the radiolabelled product and radionuclide impurity (iodine-131), respectively. The percentage of the radiochemical purity (RCP) of the radiolabelled compunds was measured by dividing the radioactivity corresponding to each compound with the total radioactivity measured on the stationary phase.

Computational Analysis

Androgen receptor (AR) and prostate-specific membrane antigen (PSMA), as well as the ligands (s-3-(4-fluorophenoxy)-2-hydroxy-2-methyl-n-[4-nitro-3-(trifluoromethyl)phenyl]propenamide/FHM, and PSMA-1007/9OT were extracted from RCSB Protein Data Bank ID: 2axa (Bohl et al., 2005), 5o5t (Cardinale et al., 2020). Isolates K7R and MRC as well as iodinated isolates K7RI and MRCI were constructed using a molecule editor software Avogadro, then positioned into receptors binding pocket using Autodock Vina (Trott & Olson, 2010). The procedures were validated using FHM and 9OT for each receptor. The binding scores of targeted compounds were compared to binding scores of those ligands. Molecular dynamic (MD) simulations were used for PSMA-K7R and PSMA-K7RI which had the highest binding score than other complexes.

The best conformation of targeted ligands K7R and K7RI in the PSMA protein pocket was

taken as initial systems for molecular dynamic (MD) study using AMBER 20 software (D.A. Case et al., 2020). Each complex systems were neutralized and solvated by TIP3P water inside 10 Å cubic box. The minimization, heating, and equilibration steps were conducted before MD production. MD simulations of complexes were performed in a constant pressure (1 atm) and temperature (310 K) by 50,000,000 iterations with dt=0.002 which were equal to 100 ns. AMBER built-in tools (cpptraj) were used in calculating Root Mean Square Deviation (RMSD) and Root Mean Square Fluctuation (RMSF) from MD trajectories. Binding affinities of ligands obtained from Autodock Vina were used for comparing binding strengths before and after MD simulations. The position and interactions of ligands in receptors were generated by using visualization softwares such as Discovery Studio Visualizer and VMD software.

Physical and ADMET properties of targeted compounds were predicted using ADMET 2.0 (Xiong et al., 2021). Online prediction simulation was used to determine absorption (Caco-2 Permeability, MDCK Permeability, Pgp-inhibitor, Pgp-substrate, HIA, F20%, and F30%), distribution (PPB, VD, BBB Penetration, and Fu), metabolism (CYP1A2, CYP2C19, CYP2C9, CYP2D6, and CYP3A4), and excretion (Cl, and T1/2). This also helped to evaluate toxicity (hERG Blockers, H-HT, DILI, AMES Toxicity, Rat Oral Acute Toxicity, FDAMDD, Skin Sensitization, Carcinogenicity, Eye Corrosion, Eye Irritation, Respiratory Toxicity, and Environmental Toxicity) as well as Tox21 Pathway (NR-AR, NR-AR-LBD, NR-AhR, NR-Aromatase, NR-ER, NR-ER-LBD, NR-PPAR-gamma, SR-ARE, SR-ATAD5, SR-HSE, SR-MMP, and SR-p53).

Statistical Analysis

The cytotoxicity and cellular uptake data were analyzed with the GraphPad Prism 9.0.0 software. Additionally, the mean ± standard deviation (SD) was used to determine viability of cell, and a paired t-test was conducted to analyze the cellular uptake data. The statistical significance of the t-test was $p<0.01$ and the confidence level was 99%.

RESULT AND DISCUSSION

Cytotoxicity Assay

In vitro biological activity was evaluated in this study through the MTT assay and cellular uptake. The MTT assay was used to determine the cytotoxicity of MRC and K7R isolated from the leaves of *M. azedarach* against human cancer cell lines, specifically LNCaP, MCF-7, and MDA-MB-231. The results showed that the viability of cells was correlated linearly with the concentration of the compounds (Figure 1). As shown in Figure 1C, after 24 hours of treatment, each compound had a distinct potential to inhibit 50% of growth cells in a cancer cell model. The National Cancer Institute (NCI) of the United States categorized cytotoxic activity as moderate when the IC_{50} ranged from 21 to 250 µg/mL (Damasuri et al., 2020), suggesting that MRC and K7R had moderate cytotoxicity. The inhibitory activity of K7R against all used cell lines was over two times more potent than MRC activity. The highest cytotoxic activity K7R against LNCaP cell lines was 154.75 µM. However, the potential cytotoxicity of this isolate increased significantly compared to the crude methanol extract of *M. azedarach* with cell viability remaining above 50% at concentrations of 750 µg/mL in LNCaP, MCF-7, and MDA-MB-231 (Nugraha et al., 2023).

Other studies reported that the kaempferol group showed anticancer potential in a variety of malignancies, including prostate and breast cancer (Shahbaz et al., 2023). Kaempferol could inhibit the growth of androgen-sensitive LNCaP cells by various pathways. This compound is capable of inhibiting the activation of AR on LNCaP cells and reduce PSA levels (Crocetto et al., 2021; Wang et al., 2021). Additionally, kaempferol directly promoted nuclear translocation process of the AR in LNCaP cells (androgen-dependent). AR is essential for the survival and proliferation of androgen-sensitive prostate cell lines, such as PSMA (Yang et al., 2005). Moreover, PSA levels are correlated with increased proliferation and a decreased apoptosis index (Niu et al., 2008).

Kaempferol has been reported with the potential to arrest the cycle in breast cancer cell lines at the G2/M phase, induce DNA damage, and trigger apoptosis by increasing the expression of caspase 3/9 and γH2AX (Shahbaz et al., 2023; Wang et al., 2019). The stated potential proves that kaempferol-type compound, including K7R, can inhibit cell proliferation. This study found that MRC and K7R showed anticancer drug potential, as evidenced by the IC_{50} value corresponding with previous reports.

Radiolabelling and Cellular Uptake

MRC and K7R have been successfully labelled with iodine-131 to produce [^{131}I]I-4-methoxyresorcinol (MRCI) and [^{131}I]I-kaempferol 7-O-rutinoside (K7RI) in good radiochemical yields (above 90%) (Figure 2).

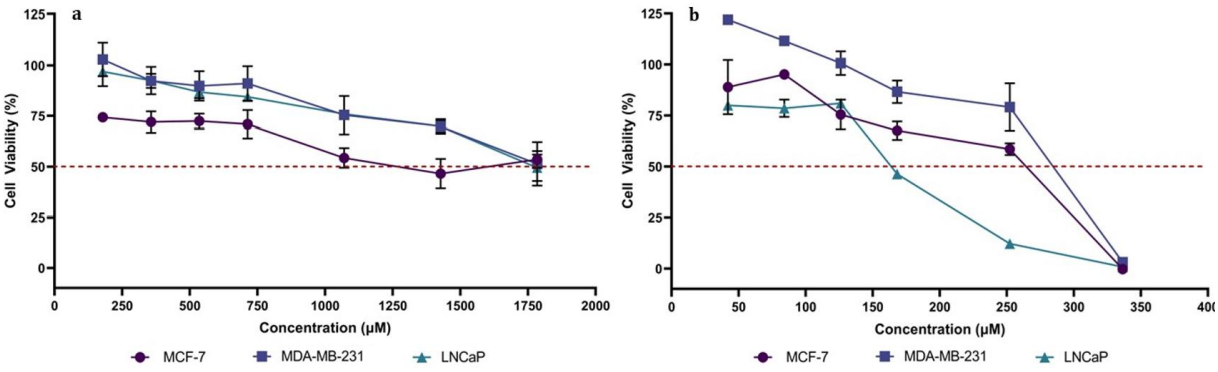

c

Compound	IC_{50} LNCaP (μM)	IC_{50} MCF-7 (μM)	IC_{50} MDA-MB-231 (μM)
4-methoxyresorcinol	1841.06	1347.19	1962.66
Kaempferol 7-O-rutinoside	154.75	221.12	235.59

Figure 1. The graph showed dose-dependent growth inhibitory activity on all cancer cell lines by MRC (a) and K7R (b), and their IC_{50} values (c).

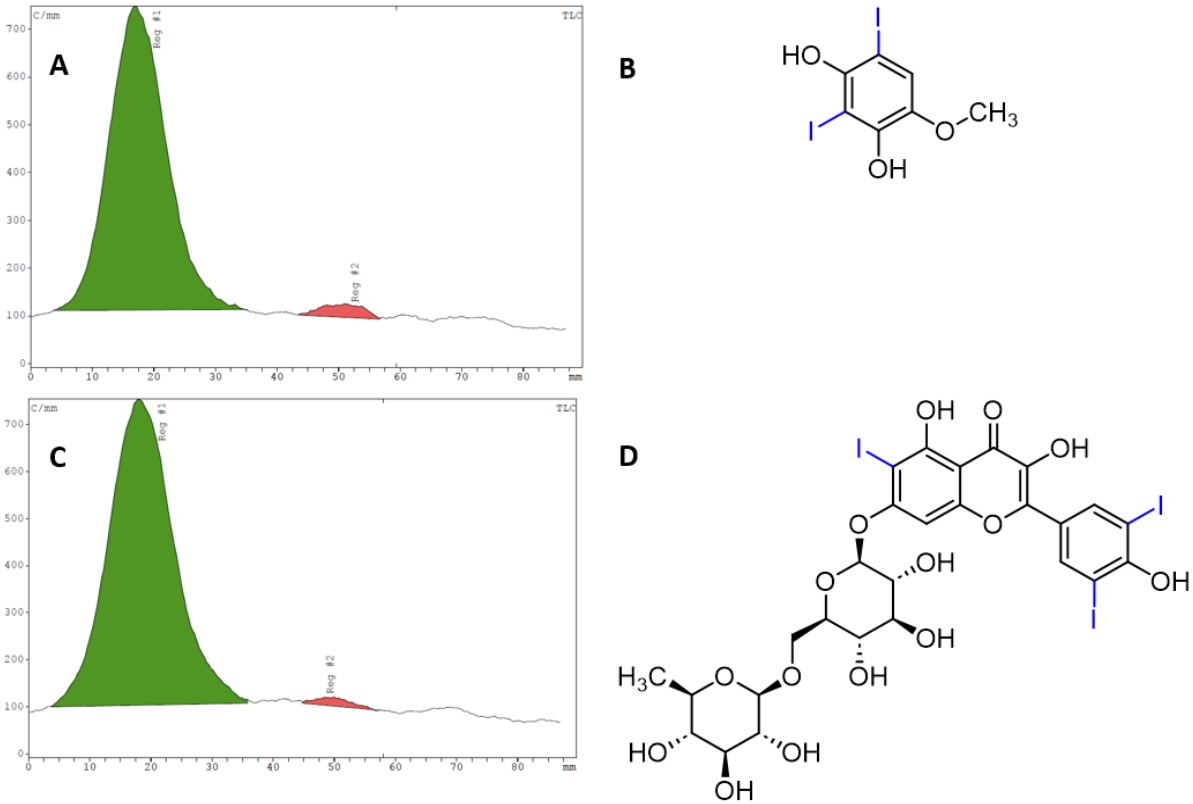

Figure 2. Radiochromatogram and the possible attachment of the radioiodine (iodine-131) atom (s) after radiolabelling under acidic conditions: MRCI (A, B) and K7RI (C, D). Green areas represent the radiolabelled compounds, while the red denotes the radionuclide impurities (free iodine-131).

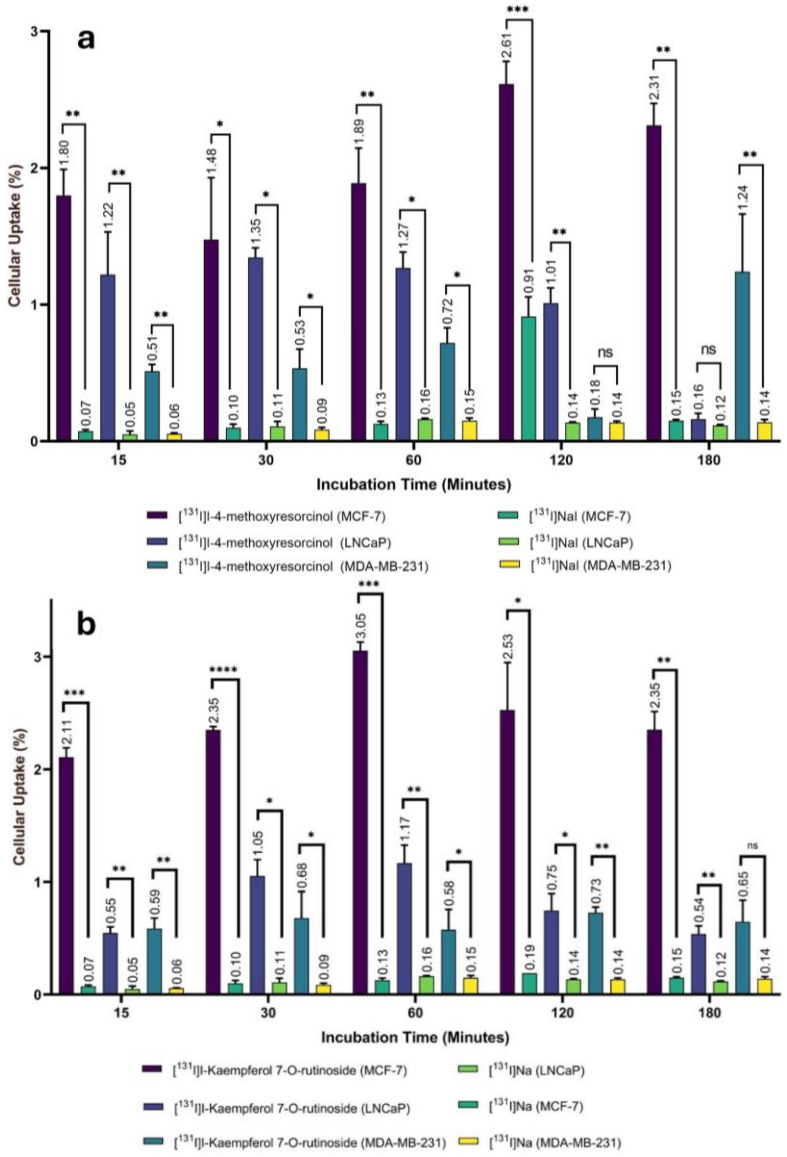

Figure 3. Cellular uptake of MRCI (A) and K7RI (B) after 0.25- to 24-hours incubation with LNCaP, MCF-7, and MDA-MB-231. The graph shows the radiolabelled compound uptake is different significantly compared to [^{131}I]NaI in nearly all cell lines.

The radioiodination of resorcinol and kaempferol was achieved through electrophilic substitution by exchanging the hydrogen with an iodine atom at the aromatic ring (s) (Figure 2).

Cell uptake studies have been performed to determine the quantity of both samples entering the cells. The results showed that the tested compounds could be internalized into cells at significantly different levels compared to iodine-131 (Figure 3). Compared to other cells, the MCF-7 had the highest uptake for both radiolabelled compounds. The highest cellular accumulation of MRCI was observed in MCF-7 (3.17±0.11%) after 24 h of incubation, approximately 20-folds greater than the control group uptake (iodine-131). Additionally, K7RI demonstrated the highest uptake in MCF-7 (3.05 ± 0.9%) after one hour of incubation, which was 23-folds higher than iodine-131 uptake.

A

Ligands	Binding score (kcal/mol)	
	AR	PSMA
FHM (AR), 9OT (PSMA)	-10.8	-10.6
Kaempferol-7-0-rutinosida	- 2.4	-10.6
Kaempferol-7-0-rutinoside_I	3.1	-11.0
4-metoksiresorsinol	-5.9	-6.1
4-metoksiresorsinol_I	-6.2	-6.1

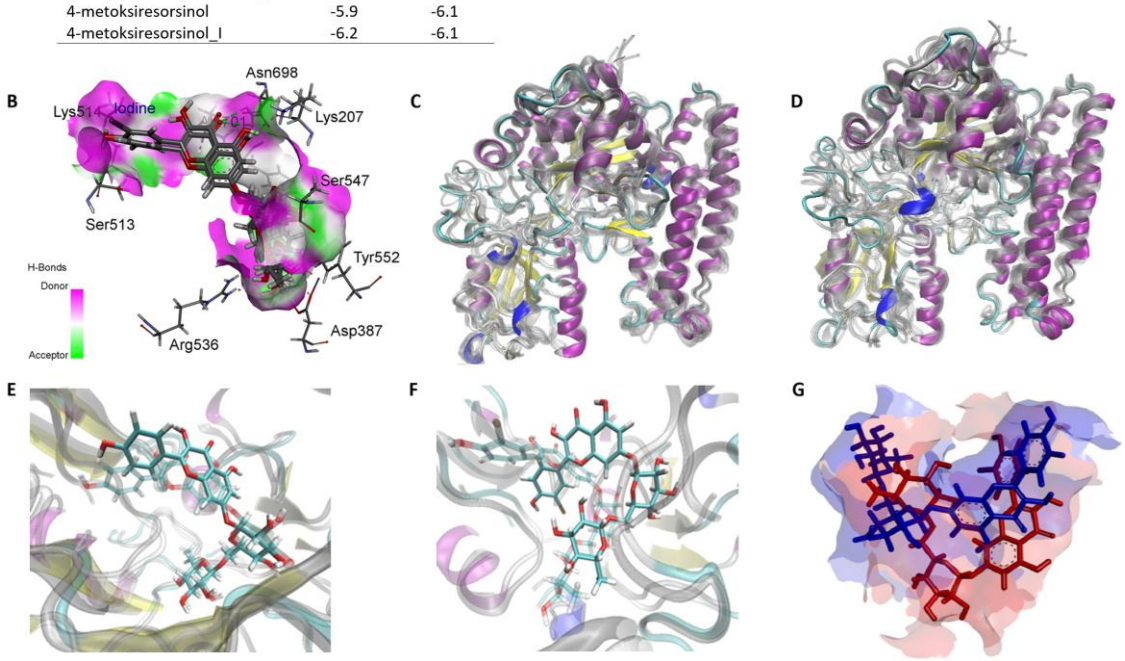

Figure 4. Binding scores of targeted ligands on prostate cancer receptors (A), K7R and K7RI on PSMA binding pocket (B), protein movement of complexes: PSMA-K7R (C) and PSMA-K7RI (D), dynamics of ligands K7R (E) and K7RI (F) from 20 ns (transparent) to 100 ns (opaque), and molecular overlay of K7R (blue) and K7RI (red) on PSMA surface after MD simulations (G).

Radiolabelled compounds in each cell showed different uptake levels during incubation, suggesting that the cells had varying sensitivities to radioiodinated compounds. These sensitivities can be attributed to a variety of factors, including the receptors in the appropriate cell lines, proapoptotic genes, ligand characteristics, and efflux phenomenon (Elliyanti et al., 2016; Kim et al., 2013; Prihatiningsih et al., 2022).

The general uptake of the radiolabeled compounds by all cells was statistically different from the uptake of the iodine-131. These results showed that the compounds can effectively bind to cancer cells. Despite that the uptake assay can help determine the degree of tracer internalization into cells and the method of action, the International Atomic Energy Agency has not established a specific threshold for the percentage of in vitro cellular uptake (IAEA, 2023). More studies are needed to comprehensively investigate and understand the mechanisms of MRCI and K7RI as radiopharmaceutical candidates.

Computational Analysis

Cytotoxicity study showed that K7R had higher activity against LNCaP compared to MCF-7 and MDA-MB-231 cell lines. The activity was confirmed by through computational studies including molecular docking and dynamics simulation of MRC, K7R, and the radioiodinated versions in some receptors expressed in LNCaP cells. Docking simulations of the investigated compounds into the active site of two receptors were conducted (Figure 4A). Docking validations were carried out by re-docking 9OT and PSMA-1007 into AR and PSMA receptors, respectively.The conformation of the ligands obtained from docking simulations had good similarity with the conformation in data bank shown as low RMSD values below 2 A°, suggesting that the docking procedures were valid. K7R was unfavourable to bind with AR, but it strongly bound to PSMA. Docking score of K7R were identical with 9OT on PSMA, and MRC had a significantly lower binding score.

Table I. ADME properties of targeted compounds

ADME Parameter	Targeted compounds			
	K7R	K7RI	MRC	MRCI
Adsorption				
Caco-2 Permeability	🔴	🔴	🟢	🟢
MDCK Permeability	🟢	🟢	🟢	🟢
Pgp-inhibitor	🟢	🟢	🟢	🟢
Pgp-substrate	🔴	🔴	🟢	🟢
HIA	🔴	🔴	🟢	🟢
$F_{20\%}$	🟢	🟢	🟢	🟢
$F_{30\%}$	🔴	🔴	🟢	🟢
Distribution				
PPB	🟢	🟢	🟢	🟢
VD	🟢	🟢	🟢	🟢
BBB Penetration	🟢	🟢	🟢	🟢
Fu	🟢	🟢	🟢	🟢
Metabolism				
CYP1A2 inhibitor	---	--	+	+++
CYP1A2 substrate	---	---	++	+++
CYP2C19 inhibitor	---	---	--	---
CYP2C19 substrate	---	---	--	--
CYP2C9 inhibitor	---	---	---	--
CYP2C9 substrate	--	---	+++	++
CYP2D6 inhibitor	---	--	--	+
CYP2D6 substrate	--	--	++	++
CYP3A4 inhibitor	---	---	--	---
CYP3A4 substrate	---	---	--	--
Excretion				
CL	🔴	🔴	🟢	🟢
$T_{1/2}$	0.694	0.520	0.916	0.847

MRC had stronger interaction with AR but showed extremely weaker interaction to FHM. Considering this perspective, K7R was more potent than MRC in prostate cancer therapy. The preferred mechanism of therapy was by inhibiting PSMA receptor. K7R interacted through H-bonds with Lys207, Asn698, Ser513, and Tyr552, as well as by hydrophobic interactions with Lys514 and Ala701. Iodination on K7R ring (K7RI) marginally affected binding affinity, which reduced binding score on AR and slightly increased binding score on PSMA. The phenolic group of K7RI interacted with Lys 514 and K7R bound to Ser513 on PSMA. The molecular overlay between K7R and K7RI (Figure 4B).

MD simulations of PSMA-K7R and PSMA-K7RI complexes for 100 ns showed insignificant movement of protein (Figure 4C-D). The average RMSD for PSMA-K7R was 2.0032 Å and RMSD during final simulation was 2.1913 Å compared to initial conformation of PSMA protein. PSMA-K7RI complexes showed higher RMSD of 2.5753 Å (average) and 2.9291 Å (100 ns). All protein residues of PSMA-K7R complexes were stable as signified by the low RMSF values (< 2A), except Val154 and Ala284 (about 3 Å). PSMA-K7R complex showed more fluctuation on Pro237, Gly263, Tyr277, Ala284, Glu489, and Thr543 with RMSF exceeding 2 Å. These residues were different from the key residues for the interactions with ligands and not located in the binding pocket area.

The MD simulations showed that K7R and K7RI had excellent stability in PSMA binding pocket for 100 ns. There were slight differences on ligand position, binding affinity, and interaction profile of ligands with protein post MD simulation (Figure 4E-F). The K7R movement around the pocket increased docking score from -10.6 to -19.5 kcal/mol. Hydrogen bond interactions occurred

with Glu457, Ser454, Arg 463, Lys514, Arg536, Ser547, Gly548, Tyr549, and Asn698, as well as hydrophobic interactions with Trp541, Tyr700 and Ala701. K7RI had significantly increased binding affinity post MD (-11.0 to -14.5 kcal/mol) but showed lower binding strength than K7R. Less protein residues participating in hydrogen bond interactions were observed in K7RI. Residues of Asp233, Glu457, Ser157, Arg534, and Ser547 provided h-bond, while Phe209, Tyr549, Tyr552, Tyr700, and Ala701 offered hydrophobic connections, and iodine reacted with Phe209 through Pi-alkyl interaction (Figure 4G). ADMET prediction results (Table I) showed poor intestinal permeability and adsorption of K7R, as well as MRC with good adsorption, distribution, and excretion properties. However, MRC might inhibit CYPs, leading to significant effects on drug response. Iodination of K7R structure did not alter these properties, while MRC iodination could change the strength of interactions with CYPs.

K7R and K7RI were both found to have the probability of being genotoxic and hepatotoxic. Based on the toxicophore of this simulation, iodine on the phenolic group of K7R only contributed to non-genotoxic carcinogenicity. K7R and K7RI showed potential to disrupt processes in the human body that may lead to negative health effects through several pathways, such as NR-AhR, NR-Aromatase, NR-PPAR-gamma, and SR-p53. Another isolate, MRC, was predicted to be harmful to the skin and eye, as well as capable of interrupting NR-AhR, NR-ER-LBD and SR-HSE pathways. MRCI was predicted to influence the SR-MMP pathways (Table I).

CONCLUSION

In conclusion, flavonoid compounds MRC and K7R were successfully isolated in this study from *M. azedarach* leaves and further radioiodinated to produce new MRCI and K7RI. Both MRC and K7R showed moderate activity against MCF-7, MDA-MB-231, and LNCaP cancer cells. Additionally, MRCI and K7RI were subjected to cellular uptake assay, which showed these two radiolabelled compounds potentially entered the cancer cells MCF-7, MDA-MB-231, and LNCaP. The computational study found that K7R had potential for prostate cancer therapy by inhibiting or interacting with PSMA. Although iodination slightly affected the affinity, interaction profile, and stability of ligands on the PSMA receptor, the radioiodinated version was predicted to produce biological activity in cancer. More investigations should be conducted to understand the molecular mechanisms that the isolated compounds use in acting against cancer cells.

ACKNOWLEDGMENT

The authors are grateful to the Directorate of Nuclear Facility Management, the radioisotope production team, the colleagues at the Multipurpose Reactor-G.A. Siwabessy, as well as the Radioisotope Research Group, Research Center for Radioisotope, Radiopharmaceutical, and Biodosimetry Technology, National Research and Innovation Agency, for the support and generosity in providing iodine-131.

FUNDING

Funding was provided by the Research Organization for Health, National Research and Innovation Agency (BRIN) under the Drug and Vaccine Development Programmes (grant number 16/III.9/HK/2023).

CONFLICT OF INTEREST

The authors declare no competing financial interests or personal relationships that could influence this study.

REFERENCES

Atanasov, A. G., Zotchev, S. B., Dirsch, V. M., International Natural Product Sciences, T., & Supuran, C. T. (2021). Natural products in drug discovery: advances and opportunities. *Nature Rev Drug Discovery,* 20, 200-216. https://doi.org/10.1038/s41573-020-00114-z

Bohl, C. E., Miller, D. D., Chen, J., Bell, C. E., & Dalton, J. T. (2005). Structural basis for accommodation of nonsteroidal ligands in the androgen receptor. *J Biol Chem,* 280, 37747-37754. https://doi.org/10.1074/jbc.M507464200

Cardinale, J., Roscher, M., Schafer, M., Geerlings, M., Benesova, M., Bauder-Wust, U., Remde, Y., Eder, M., Novakova, Z., Motlova, L., Barinka, C., Giesel, F. L., & Kopka, K. (2020). Development of PSMA-1007-related series of ^{18}F-labeled Glu-Ureido-type PSMA inhibitors. *J Med Chem,* 63, 10897-10907. https://doi.org/10.1021/acs.jmedchem.9b01479.s002

Crocetto, F., di Zazzo, E., Buonerba, C., Aveta, A., Pandolfo, S. D., Barone, B., Trama, F., Caputo, V. F., Scafuri, L., Ferro, M., Cosimato, V., Fusco, F., Imbimbo, C., & Di Lorenzo, G. (2021).

Kaempferol, myricetin and fisetin in prostate and bladder cancer: a systematic review of the literature. *Nutrients,* 13, 3750. https://doi.org/10.3390/nu13113750

D.A. Case, K. Belfon, I.Y. Ben-Shalom, S.R. Brozell, D.S. Cerutti, T.E. Cheatham, V.W.D. Cruzeiro, T.A. Darden, R.E. Duke, G. Giambasu, M.K. Gilson, H. Gohlke, A.W. Goetz, R. Harris, S. Izadi, S.A. Izmailov, K. Kasavajhala, A. Kovalenko, R. Krasny, T. Kurtzman, T.S. Lee, S. LeGrand, P. Li, C. Lin, J. Liu, T. Luchko, R. Luo, V. Man, K.M. Merz, Y. Miao, O. Mikhailovskii, G. Monard, H. Nguyen, A. Onufriev, F. Pan, S. Pantano, R. Qi, D.R. Roe, A. Roitberg, C. Sagui, S. Schott-Verdugo, J. Shen, C.L. Simmerling, N.R. Skrynnikov, J. Smith, J. Swails, R.C. Walker, J. Wang, L. Wilson, R.M. Wolf, X. Wu, Y. Xiong, Y. Xue, D.M. York, & Kollman, P. A. (2020). AMBER 2020, University of California, San Francisco.

Damasuri, A. R., Sholikhah, E. N., & Mustofa. (2020). Cytotoxicity of ((E)-1-(4-aminophenyl)-3-phenylprop-2-en-1-one)) on HeLa cell line. *IJPTher,* 1, 54-59. https://doi.org/10.22146/ijpther.606

Debela, D. T., Muzazu, S. G., Heraro, K. D., Ndalama, M. T., Mesele, B. W., Haile, D. C., Kitui, S. K., & Manyazewal, T. (2021). New approaches and procedures for cancer treatment: Current perspectives. *SAGE Open Medicine,* 9, 20503121211034366. https://doi.org/10.1177/20503121211034366

Elliyanti, A., Susilo, V. Y., Setiyowati, S., Ramli, M., Masjhur, J. S., & Achmad, T. H. (2016). Uptake and Cytotoxicity Characterization of Radioiodine in MCF-7 and SKBR3 Breast Cancer Cell Lines. Atom Indonesia, 42(3), 145. https://doi.org/10.17146/aij.2016.586

Hanif, N., Murni, A., Tanaka, C., & Tanaka, J. (2019). Marine natural products from Indonesian waters. *Mar Drugs,* 17, 364. https://doi.org/10.3390/md17060364

IAEA. (2023). *Guidance for Preclinical Studies with Radiopharmaceuticals*. www.iaea.org/publications

J. Zhao, L. Xu, J. Sun, M. Song, L. Wang, S. Yuan, Y. Zhu, Z. Wan, S. Larsson, K. Tsilidis, M. Dunlop, H. Campbell, I. Rudan, P. Song, E. Theodoratou, K. Ding, & X. Li. (2023). Global trends in incidence, death, burden and risk factors of early- onset cancer from 1990 to 2019. *BMJ Oncology*, 2, e000049. https://doi.org/10.1136/bmjonc-2023-000049

Kim, H. W., Kim, J. E., Hwang, M.-H., Jeon, Y. H., Lee, S.-W., Lee, J., Zeon, S. K., & Ahn, B.-C. (2013). Enhancement of Natural Killer Cell Cytotoxicity by Sodium/Iodide Symporter Gene-Mediated Radioiodine Pretreatment in Breast Cancer Cells. PLoS ONE, 8(8), e70194. https://doi.org/10.1371/journal.pone.0070194

Menez, R., Michel, S., Muller, B. H., Bossus, M., Ducancel, F., Jolivet-Reynaud, C., & Stura, E. A. (2008). Crystal structure of a ternary complex between human prostate-specific antigen, its substrate acyl intermediate and an activating antibody. *J Mol Biol, 376*, 1021-1033. https://doi.org/10.1016/j.jmb.2007.11.052

Mosmann, T. (1983). Rapid colorimetric assay for cellular growth and survival: application to proliferation and cytotoxicity assays. *J Immunol Methods,* 65, 55-63. https://doi.org/10.1016/0022-1759(83)90303-4

Nasim, N., Sandeep, I. S., & Mohanty, S. (2022). Plant-derived natural products for drug discovery: current approaches and prospects. *Nucleus (Calcutta),* 65, 399-411. https://doi.org/10.1007/s13237-022-00405-3

Niu, Y., Yeh, S., Miyamoto, H., Li, G., Altuwaijri, S., Yuan, J., Han, R., Ma, T., Kuo, H. C., & Chang, C. (2008). Tissue prostate-specific antigen facilitates refractory prostate tumor progression via enhancing ARA70-regulated androgen receptor transactivation. *Cancer Res,* 68, 7110-7119. https://doi.org/10.1158/0008-5472.CAN-07-6507

Nugraha, A. S., Firli, L. N., Hendra, R., Keller, P. A., Purwoko, R. Y., Idrus, H. H., Ritawidya, R., Febrian, M. B., Mahendra, I., Kurniawan, A., Forentin, A. M., Susilo, V. Y., Kusumaningrum, C. E., Setiadi, Y., & Wongso, H. (2023). Anticancer activity of Indonesian *Melia azedarach* L.: Phyto-chemistry, in vitro and in silico studies. *J Biol Act Prod Nat,* 13, 12-26. https://doi.org/10.1080/22311866.2023.2172079

Nugrahaa, A. S., & Keller, P. A. (2011). Revealing indigenous indonesian traditional medicine: anti-infective agents. *Nat Prod Commun,* 6, 1956-1966.

https://doi.org/10.1177/1934578x1100601240

Panche, A. N., Diwan, A. D., & Chandra, S. R. (2016). Flavonoids: an overview. *J Nutr Sci,* 5, e47. https://doi.org/10.1017/jns.2016.41

Petrov, S. A., Yusubov, M. S., Beloglazkina, E. K., & Nenajdenko, V. G. (2022). Synthesis of radioiodinated compounds. Classical approaches and achievements of recent years. *Int J Mol Sci,* 23, 1-41. https://doi.org/10.3390/genes1030413

Prihatiningsih, M. C., Ariyanto, T., Putra, E. G. R., Susilo, V. Y., Mahendra, I., & Prasetyo, I. (2022). Radioiodination of modified porous silica nanoparticles as a potential candidate of Iodine-131 drugs vehicle. *ACS Omega*, *7*(16), 13494–13506. https://doi.org/10.1021/acsomega.1c06492

Rizvi, S. A. A., Einstein, G. P., Tulp, O. L., Sainvil, F., & Branly, R. (2022). Introduction to traditional medicine and their role in prevention and treatment of emerging and re-emerging diseases. *Biomolecules,* 12, 1442. https://doi.org/10.3390/biom12101442

Shahbaz, M., Imran, M., Alsagaby, S. A., Naeem, H., Al Abdulmonem, W., Hussain, M., Abdelgawad, M. A., El-Ghorab, A. H., Ghoneim, M. M., El-Sherbiny, M., Atoki, A. V., & Awuchi, C. G. (2023). Anticancer, antioxidant, ameliorative and therapeutic properties of kaempferol. *Int J Food Prop, 26*, 1140-1166. https://doi.org/10.1080/10942912.2023.2205040

Trott, O., & Olson, A. J. (2010). AutoDock Vina: improving the speed and accuracy of docking with a new scoring function, efficient optimization, and multithreading. *J Comput Chem,* 31, 455-461. https://doi.org/10.1002/jcc.21334

Tungmunnithum, D., Thongboonyou, A., Pholboon, A., & Yangsabai, A. (2018). Flavonoids and other phenolic compounds from Medicinal plants for pharmaceutical and medical aspects: an overview. *Medicines (Basel),* 5, 93. https://doi.org/10.3390/medicines5030093

Ullah, A., Munir, S., Badshah, S. L., Khan, N., Ghani, L., Poulson, B. G., Emwas, A. H., & Jaremko, M. (2020). Important flavonoids and their role as a therapeutic agent. *Molecules,* 25, 5243. https://doi.org/10.3390/molecules25225243

Wang, X., Yang, Y., An, Y., & Fang, G. (2019). The mechanism of anticancer action and potential clinical use of kaempferol in the treatment of breast cancer. *Biomed Pharmacother,* 117, 109086. https://doi.org/10.1016/j.biopha.2019.109086

Wang, X., Zhu, J., Yan, H., Shi, M., Zheng, Q., Wang, Y., Zhu, Y., Miao, L., & Gao, X. (2021). Kaempferol inhibits benign prostatic hyperplasia by resisting the action of androgen. *Eur J Pharmacol,* 907, 174251. https://doi.org/10.1016/j.ejphar.2021.174251

Wongso, H. (2022). Natural product-based radiopharmaceuticals: Focus on curcumin and its analogs, flavonoids, and marine peptides. *J Pharm Anal,* 12, 380-393. https://doi.org/10.1016/j.jpha.2021.07.006

Wongso, H., Nuraeni, W., & Rosyidiah, E. (2022). Efficient and practical radiosynthesis of novel [^{131}I]-Xanthine and [^{131}I]-hypoxanthine. *At. Indones,* 48, 185. https://doi.org/10.17146/aij.2022.1233

Xiong, G., Wu, Z., Yi, J., Fu, L., Yang, Z., Hsieh, C., Yin, M., Zeng, X., Wu, C., Lu, A., Chen, X., Hou, T., & Cao, D. (2021). ADMETlab 2.0: an integrated online platform for accurate and comprehensive predictions of ADMET properties. *Nucleic Acids Res,* 49(W1), W5-W14. https://doi.org/10.1093/nar/gkab255

Yang, Q., Fung, K. M., Day, W. V., Kropp, B. P., & Lin, H. K. (2005). Androgen receptor signaling is required for androgen-sensitive human prostate cancer cell proliferation and survival. *Cancer Cell International, 5*, 8. https://doi.org/10.1186/1475-2867-5-8